

Original Research

Activated Persulfate by Dielectric Barrier Discharge Plasma for the Degradation of Unsymmetrical Dimethyl Hydrazine as Wastewater Pollutants

Zhen Zhou¹, Zhi Zheng^{1*}, Huijun Li¹, Ren He¹, Ruiqin Hou¹, Yaqin Yu², Yao Yang¹

¹State Key Laboratory of Technologies in Space Cryogenic Propellants, Beijing Special Engineering Design and Research Institute, Beijing 100028, China

²Center for Environmental Metrology, National Institute of Metrology, Beijing 100029, China

Received: 7 December 2022

Accepted: 2 February 2023

Abstract

Releasing unsymmetrical dimethyl hydrazine (UDMH) in ambient medium is an escalating environment crisis that catches aggrandizing public concerns. Herein, a non-thermal plasma activating persulfate maneuver was introduced and its application mechanism in UDMH degradation was explored. Oxidizing kinetic experiments show that 93.8% UDMH were eliminated along with 12.5 kV, pH = 8, 50 mM NaCl, $\text{Na}_2\text{S}_2\text{O}_8/\text{UDMH}$ (mol/mol) = 2, and 140 mL/min. The Visual MINTEQ simulated species distribution of UDMH well predicted the oxidation behaviors of UDMH in the variation of pH. Radical scavenging test integrated with UV-vis spectroscopy were introduced to identify the predominating reactive oxygen species during UDMH decomposition. The $\cdot\text{OH}$ and $\cdot\text{SO}_4^-$ played a synergistic role in the UDMH oxidization. Overall, this study may shed new lights on the degradation of UDMH industry wastewater using hybrid technique.

Keywords: non-thermal plasma, persulfate, unsymmetrical dimethyl hydrazine, species distribution

Introduction

In the wake of explosive development of space technology, a huge amount of propellant wastewater was engendered. It was documented that 300-600 tons wastewater was acquired in each rocket lunch [1]. There is a gradual alleviation in ambient conditions after the emerging of cryogenic propellants. However,

the conventional propellants are unavoidable especially in posture alignment [2]. Unsymmetrical dimethyl hydrazine (UDMH) combined with nitrogen tetroxide represent some of the most common bipropellant. Owing to its high stability and excellent specific impulse, UDMH have garnered enormous heed in aerospace industry and military field [3]. The preponderance of UDMH intrigue a wide application to the gamut of semiconductor manufacturing, drug and dye intermediates industry, polymerization catalysis and so forth [4].

*e-mail: 13793182581@163.com

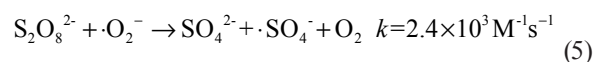
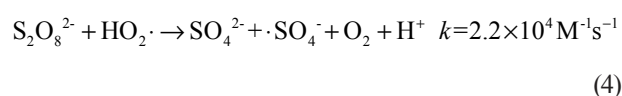
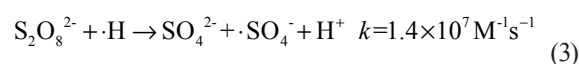
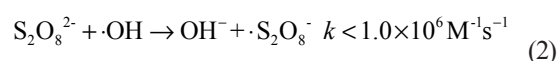
Pending a period of groping, it has been stepwise endorsed that UDMH play a suspected role in severe abnormalities, such as cancer and neurotoxicity [3, 5]. Besides that, inhalation of UDMH results in Vitamin B6 deficiency disease. Hence, dealing with UDMH pollution has been of great concern owing to inherent toxicity of UDMH to environments and human health. Heretofore, adsorption, ion exchange, biological method, advanced oxidation processes (AOPs) have been employed as instrumentalities for UDMH polluted wastewater purification. Nevertheless, the practical application of above methods were hindered by their inherent demerits [3, 6-9].

Among them, sulfate radical based-AOPs are putative in a catchy approach [10-12]. The main source of sulfate radical is come from persulfate. Normally, the oxidation efficacy (1.96-2.01 V) of pollutants via persulfate straightforwardness is inferior [7]. With the collaboration of heat, bases, microwave, carbon materials, transition metals, and ultraviolet light, enhancement in pollutants oxidation were obtained [13, 14].

When a high voltage crossed through the positive and negative electrode, ionizable electrons deriving from electric discharge will be triggered. Subsequently, exuberant chemical and physical influence about discharge electric field, ultraviolet light, and shock waves have been engendered since the inelastic collisions between the ionized electrons, atoms, and molecules [15, 16]. The preponderance of dielectric barrier discharge (DBD) plasma is pertinent to its discharge stability and controllability, which makes it to be one of the most common strategy in non-thermal plasma wastewater treatment [17].

Latterly, nanosecond pulsed discharge based plasma have been investigated to eliminate acid red 73, following 83.2% degradation in 30 min [18]. A document released by Rong et al. illustrated that 85.74% of 1 g/L polyacrylamide wastewater was oxidized by non-thermal plasma in 5 h [16]. Liu and coworkers [15] have employed DBD plasma to treat wastewater containing Cr(VI). The reductive $\cdot\text{H}$ and oxidative $\cdot\text{OH}$, generation from DBD plasma, reduce Cr(VI) and oxidize phenol, respectively. Recently, it has been stepwise endorsed that utilization DBD plasma to handle industrial water directly rendering the thorny bottlenecks: superior energy consumption and inferior electrical utility.

The DBD plasma rendered ozonation, shock waves, and ultraviolet light radiation inspired us to delve into the combination of DBD plasma and persulfate. The combined physical and chemical agents of DBD plasma activate persulfate (Eq. 1-5) without further chemical additions, which furtherly induce various reactive species ($\cdot\text{O}$, $\cdot\text{OH}$, O_3 , H_2O_2 , etc.) [19], and devastating the refractory contaminants.



Consequently, it is incumbent on us to combined DBD plasma with persulfate in UDMH wastewater treatment. Macroscopic oxidation kinetics, UV-vis spectroscopy, and the Visual MINTEQ simulation were systematic conducted to optimize the hybrid reaction parameters and explore oxidizing mechanism. This investigation would provide an essential observation in the broader spectrum of industrial wastewater treatment and deeper understanding of UDMH oxidizing mechanism.

Material and Methods

Materials

We purchased 98.7% UDMH in mass ratio from the Beijing institute of aerospace testing technology. Barring the $\text{K}_2\text{Cr}_2\text{O}_7$ in superior grade, $\text{Na}_2\text{S}_2\text{O}_8$, NaCl , NaOH , HgSO_4 , Ag_2SO_4 , $(\text{NH}_4)_2\text{Fe}(\text{SO}_4)_2 \cdot 6\text{H}_2\text{O}$, $\text{Na}_2\text{HPO}_4 \cdot 12\text{H}_2\text{O}$, $\text{Na}_2[\text{Fe}(\text{CN})_5\text{NO}] \cdot 2\text{H}_2\text{O}$, 1,10-phenanthroline, acetic acid, acetylacetone, ammonium acetate, tert-butanol, and methanol were employed in analytical grade from sinopharm chemical reagent. The absolute alcohol, citric acid, and H_2SO_4 were acquired from Beijing chemical works. Dissolution of abovementioned chemicals were conducted by ultrapure water (18.2 M Ω , Milli-Q, USA), and then refrigerated at 4°C until needed.

Apparatus

As sketched in Fig. 1, oxidation process were implement in a dielectric barrier discharge reactor, composing of a CTP-2000K plasma power supply (Nanjing Suman Plasma Technology), a MS07104B endoscope (Agilent Technologies), a CT1000 peristaltic pump (Enyi Industry), a blower, a tubular DBD reactor, and a water tank. The tubular DBD reactor is an aqueduct with concentric high-tension electrode and grounded stainless steel electrode. Two concentric quartz channels placed between discharge electrode and grounded electrode with 25 mm and 40 mm in diameter. Water in the tank was pumped into the inner quartz tube by down-to-up mode, and then the overflowed water drop into the outer quartz tube. With a concomitant discharge plasma, the processed water was gathered in the water tank. The electrolysis time was calculated by $1/4 \times \pi \times (4^2 - 2.5^2) \times 12 \div \text{circular flow (min)}$.

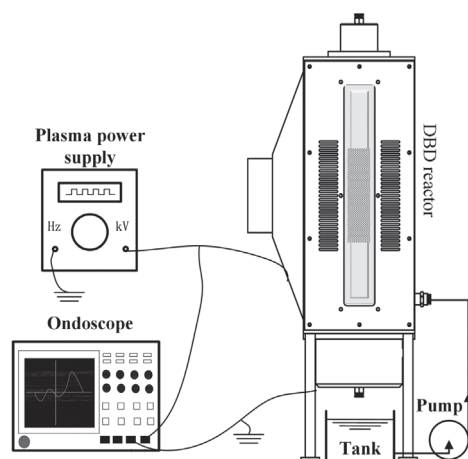


Fig. 1. Schematic illustration of experimental system.

UDMH Degradation

In synthetic UDMH wastewater systems, 50 mM NaCl was selected as background electrolyte and the UDMH concentration was fixed at 100 mg/L. Optimization protocol of pH within the purview of 4-10 were modulated by NaOH and H₂SO₄. Na₂S₂O₈ was added with a molar ratio at 0-2.5 under stirring. To evaluate the influence of discharge voltage, 20-30 kV voltages were adopted concurring 10 kHz power frequency. Flow rate covering 100-180 mL/min were controlled by peristaltic pump. During the entire test, 3 mL aliquot was collected with the time intervals 5 min (during 25 min) and 10 min (till 45 min). The collected samples was quenching by 0.1 mL alcohol to end the reaction. After appropriately dilution, aqueous UDMH content was gauged in triplicate using UV-2550 spectrophotometry (SHIMADZU) based on amino ferrocyanide sodium method.

In situ identification of pH and conductivity were monitored by HACH HQ11d and HQ14d meter, respectively. To avoid the harmful of UDMH, all operations were conducted in the fume cupboard.

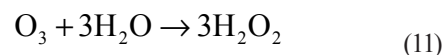
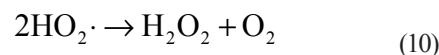
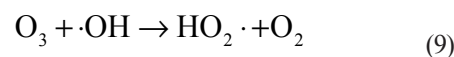
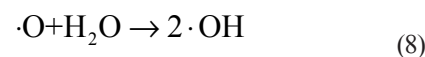
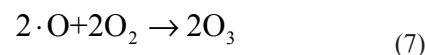
Results and Discussion

Variation of Discharge Voltage

Inset images in Fig. 2(a-c) clearly show the plasma excitation on UDMH solution. No obvious ionizing phenomenon displayed in the aqua at 10 kV peak voltage except the purple rings occurred in the upper and lower due to the air breakdown effect. The experimental observation fitting well to the data of voltage and current in Fig. 2a). With the increment of voltage, the feeble signal in solution become obvious purple silk in the inset of Fig. 2b). The vibration current located in Fig. 2b) are designated as the electricity-induced excitation, verifying the presence of plasma. Further increasing peak voltage to 15 kV, the electrical

silk extend into the whole aqueous solution, coupling with more conspicuous vibration current.

The discharge voltage is pertinent to the intensity of reactive species and its discharge stability and uniformity. All UDMH oxidation process was conducted in ambient air for expenditure-benefit balance. Effect of sparking voltage covering 0-15 kV on 100 mg/L UDMH removal was studied under 140 mL/min flow rates with Na₂S₂O₈/UDMH(mol/mol) = 1.0 and pH = 8. Fig. 2d) sketches the percentile of UDMH at different voltage covering the purview of 0-15 kV. Evidently, the oxidization kinetics of UDMH manifests an ascent curve, and 73.8% UDMH was removed in the presence of Na₂S₂O₈ and absence of electricity. This appreciable tendency was ascribed to its high oxidation potential. The oxidation potential of S₂O₈²⁻ (E₀ = 2.01 V) was commensurate with that of O₃ (E₀ = 2.08 V) which could be applied to degrade organics directly [17]. There is an appreciable mounting in the UDMH degradation from voltage-less to 12.5 kV. The enhanced oxidability was premier attributed to the enriched electron density, reactive molecules (O₃, H₂O₂) and free radicals (Eq. 6-11). Furthermore, physical effects of UV and heat under higher voltage is conducive to activate persulfate and incubate ·OH/·SO₄⁻.



Revvng voltage up to 12.5 kV has been found to be a baneful procedure to UDMH removal. The enhanced side reaction between ·SO₄⁻ and ·OH or ·SO₄⁻ and its own in excessive voltage [20] vied with UDMH for free radicals. Another explanation for above results is the higher voltage brought higher temperature, invalidating oxide capacity [21].

As plotted in Fig. 2e), the change in pH variation as a function of applied voltage was similar in the purview of 0-12.5 kV. The experimental observations highlight that the pH of aqua plummeted about 4 in the first 10 min. When time >10 min, the pH of 0-12.5 kV dwindled to 3.4 at 45 min. Nevertheless, aqueous pH descended sharper when peak voltage arrived at 15 kV. The appreciable tendency of aqueous pH between absence and presence of electricity implied that the reaction between ·SO₄⁻ and water molecule (Eq. 12) [22]

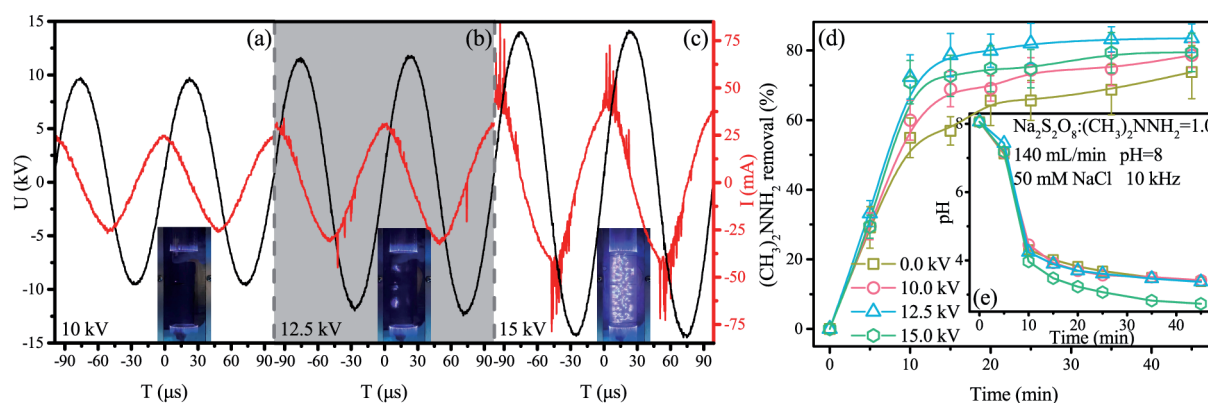
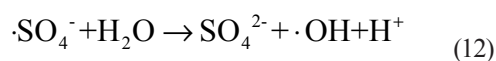


Fig. 2. (a-c) Effect of different peak voltage on current and discharge effect. d) Oxidizing kinetics of UDMH in 50 mM NaCl background at voltage 0, 10, 12.5, and 15 kV, respectively. e) The corresponding pH kinetics in the fluctuation of peak voltages.

was nonnegligible when time <10 min, whereas plasma produced NO and NO₂ in ambient air [23] made aqua more acidic in 10-45 min.



Variation of Initial pH

pH is significant to the species of UDMH, which inspires us to delve into the influence of pH in 4-10. As illustrated in Fig. 3, oxidizing kinetics of 100 mg/L UDMH at pH = 4-10 was monitored under 140 mL/min flow rates with Na₂S₂O₈/UDMH (mol/mol) = 1.0, 50 mM NaCl, and 12.5 kV.

It was found that the oxidizing percentage of UDMH was parabolic, hint that there exists an optimum range of pH value (pH 8). Before the maximum, the remaining rate of UDMH was diminished with the escalation of initial pH. When the initial pH ≥ 8, the decomposition was rapid before 15 min, and then gained equilibrium. Nonetheless, the elimination of UDMH was marginally inhibited at initial pH = 10.

The experimental observations in pH 4, 6, and 8 can be well portrayed via the Visual MINTEQ. Fig. 3c) describes the theoretical species distribution of UDMH deriving from the Visual MINTEQ 3.1. With the escalating of pH, an equilibrium point between (CH₃)₂NHNH₂⁺ and (CH₃)₂NH₂ achieved at pH 7.21. (CH₃)₂NHNH₂⁺ dominates in aqua below the balance point, and (CH₃)₂NH₂ turns into the main segment at pH above 7.21. Equations (13)-(14) [24] delineates that the neutral (CH₃)₂NH₂ degradation capacities with ·OH were 19.8-folds than that of charged (CH₃)₂NHNH₂⁺. What's more, persulfate cloud be catalyzed by H⁺ under acid circumstance which is non-radical pathway and not yielding ·SO₄⁻ [25]. Species distribution and H⁺ competition account for superior elimination behavior of pH 8 than that of pH 4 and 6.

When the pH exceeded 10, the elimination plateau of pH 10 was slightly lower than that of pH 8. A likely explanation may incriminate to the seemingly

counterintuitive results. The alkaline conditions were more accessible to transform ·SO₄⁻ and plasma-produced O₃ into ·OH via Eq. (15-16). In alkaline aqua, ·OH expressed an inferior chemical activity [22]. Besides that, transformation of ·OH to H₂O₂ and ·O⁻ (Eq. 17-18) played a deleterious role in S₂O₈²⁻ (Eq. 19) [17].

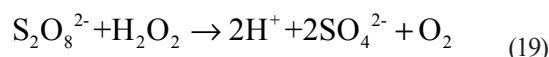
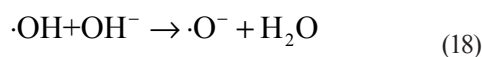
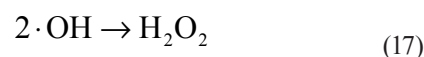
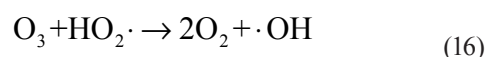
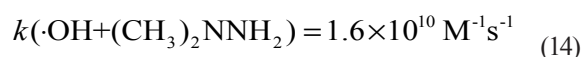
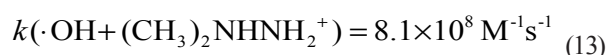


Fig. 3b) sketch the pH kinetics with a concomitant diminution of alkalinity. Barring curve of initial pH 4, evident dropping of pH to ~4 was occurred in other kinetic curves within 10 min and then dwindled in the residual time. In case of pH 4, its real-time pH descended consistently during the entire reaction, signifying lower pH precludes the UDMH oxidizing rate.

Variation of NaCl Ionic Strength

To gain oxidizing kinetics of 100 mg/L UDMH over the background electrolyte, NaCl ionic strength was varied from 0 to 100 mM for a fixed 140 mL/min flow rates with Na₂S₂O₈/UDMH (mol/mol) = 1.0 and 12.5 kV, while prolonging the reaction time to 45 min. As recorded in Fig. 4a), there are rapid decomposition

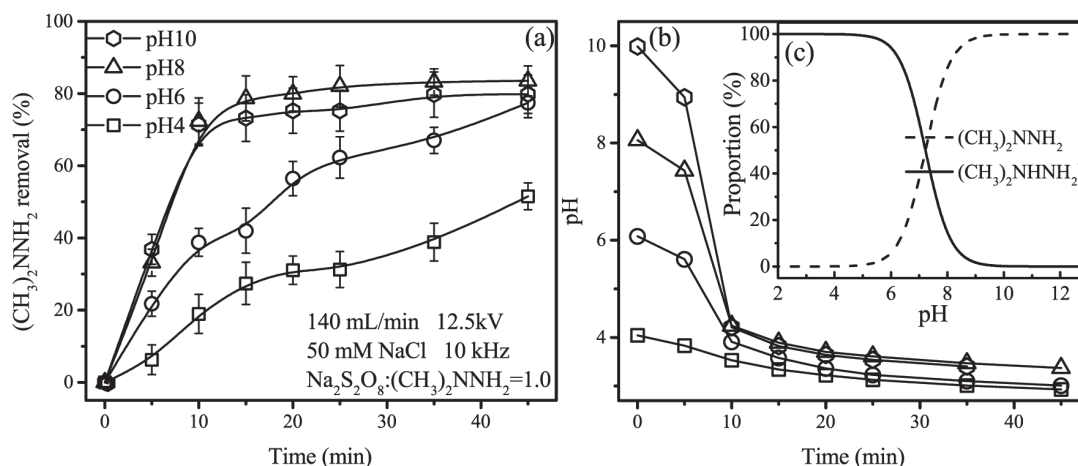
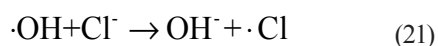
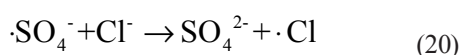


Fig. 3. a) Oxidizing kinetics of UDMH in 50 mM NaCl background at initial pH 4, 6, 8, and 10, respectively. b) The corresponding pH kinetics in the fluctuation of initial pH. c) Species distribution of UDMH under Visual MINTEQ simulation.

of UDMH before 10 min and then decelerated notably with the degradation plateau after 10 min. An ascending tendency in elimination beyond 10 min are marginal and an equilibrium is arriving. The oxidizing rate of 50 mM NaCl background system was faster than that of NaCl-less background system before ~10 min. Then, the equilibrium oxidizing capacity of the former was higher than the later (83.5% > 38.5%). NaCl addition exhibited significant synergistic effect might attribute to the generation of chlorine-containing radicals viz., HOCl, OCl⁻, ·Cl, ·Cl₂ (Eq. 20-21) [26] which was prone to attack electron-rich UDMH. However, slightly higher (<10%) UDMH oxidizing capacity occurred at 100 mM NaCl background system. Because the outrageous conductivity was detrimental in incubating intense electrical field, plasma channels, and active radicals [27].



Variation of Molar Ratio on $\text{Na}_2\text{S}_2\text{O}_8$ and UDMH

As demonstrated in Fig. 4(b-c), Oxidizing kinetics of 100 mg/L UDMH at 0-2.5 persulfate-to-UDMH ratio was scrutinized under 140 mL/min flow rates with 50 mM NaCl, pH 8, and 12.5 kV. Fig. 4b) shows that 49.9% UDMH was depleted in the $\text{Na}_2\text{S}_2\text{O}_8$ -less solution following 45 min DBD plasma treatment. In the case of $\text{Na}_2\text{S}_2\text{O}_8/\text{UDMH}$ (mol/mol) = 0.5, the oxidized percentages of UDMH boosted from 62.6% at 10 min to 65.3% at 45 min. The rapid removal of UDMH after $\text{Na}_2\text{S}_2\text{O}_8$ addition was ascribe to the catalyst of DBD plasma (Eq. 22) and the subsequently synergetic effect of ·OH and ·SO₄⁻ (Eq. 23-24) [28-30], promoting the degradation efficiency and removal rate of UDMH. The degradation efficacy elevated noticeably as the rising molar ratio (0.5-2) and then swelled slowly due to excess persulfate. Over amount of $\text{Na}_2\text{S}_2\text{O}_8$ spawned to self-annihilation (Eq. 25-27) [19], and hindered the availability of ·SO₄⁻.

As delineated in Fig. 4c), line graph of persulfate-less attained a vertex in 10 min and then decelerated

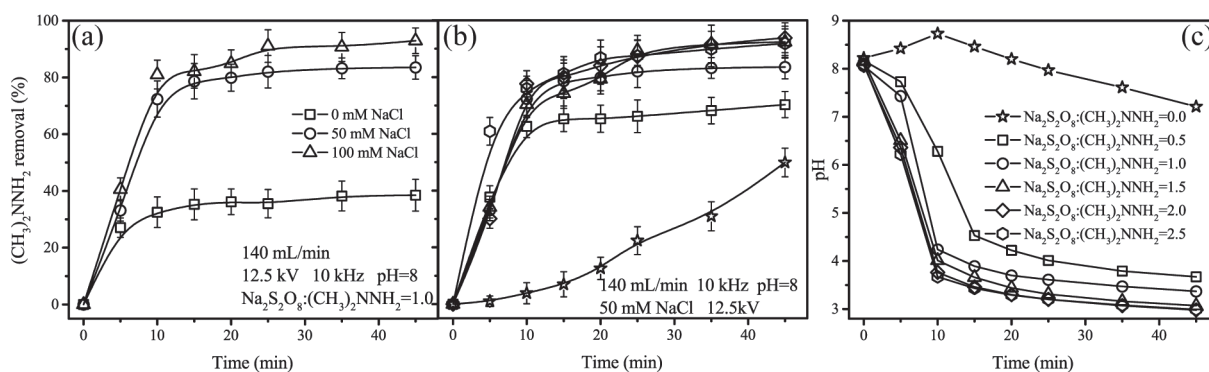
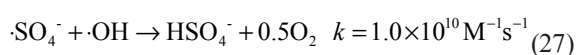
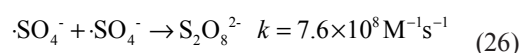
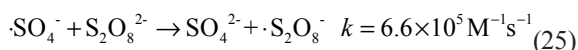
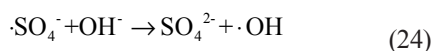
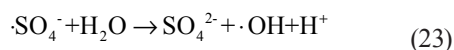
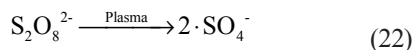


Fig. 4. a) Oxidizing kinetics of UDMH in different NaCl background electrolyte. b) Oxidizing kinetics of UDMH in 50 mM NaCl background at initial pH 8 with variation of $\text{Na}_2\text{S}_2\text{O}_8/\text{UDMH}$ (mol/mol) = 0-2.5. c) The corresponding pH kinetics in the fluctuation of molar ratio on $\text{Na}_2\text{S}_2\text{O}_8$ and UDMH.

notably with time elapsed. In terms of $\text{Na}_2\text{S}_2\text{O}_8/\text{UDMH}$ (mol/mol) = 0.5, the wastewater pH plummeted from onset to pH 4.5 at 15 min, assigning to H^+ production and OH^- consumption (Eq. 12, 24). Higher persulfate-to-UDMH ratio manifested similar pH behavior to $\text{Na}_2\text{S}_2\text{O}_8/\text{UDMH}$ (mol/mol) = 0.5, except for lower final pH.



Variation of Circular Flow

Impingement of flow rates covering 100-180 mL/min on 100 mg/L UDMH removal was implemented under 50 mM NaCl background with $\text{Na}_2\text{S}_2\text{O}_8/\text{UDMH}$ (mol/mol) = 2.0, 12.5 kV, and pH = 8. The maximum decomposition capacity for UDMH in Fig. 5a) enhanced with the increment of flow rates and obtained the summit 93.8% at 140 mL/min. In the lower flow rates, rising flow rates actuated the generation of continuous water film, which is beneficial to the formation and utilization of active substances [31]. In addition, higher flow rates resulted in an improved cycle numbers in per unit time, and thus elevated plasma-induced numbers. Notwithstanding, slightly diminution to 85.8% occurred on 180 mL/min in virtue of the unsteady gas-liquid flow in the gap between inner and outer quartz tube, which is baneful to gain active substances [31].

As illustrated in Fig. 5b), oxidizing behavior of 100-500 mg/L UDMH at persulfate-to-UDMH ratio = 2 was delved under 140 mL/min flow rates with

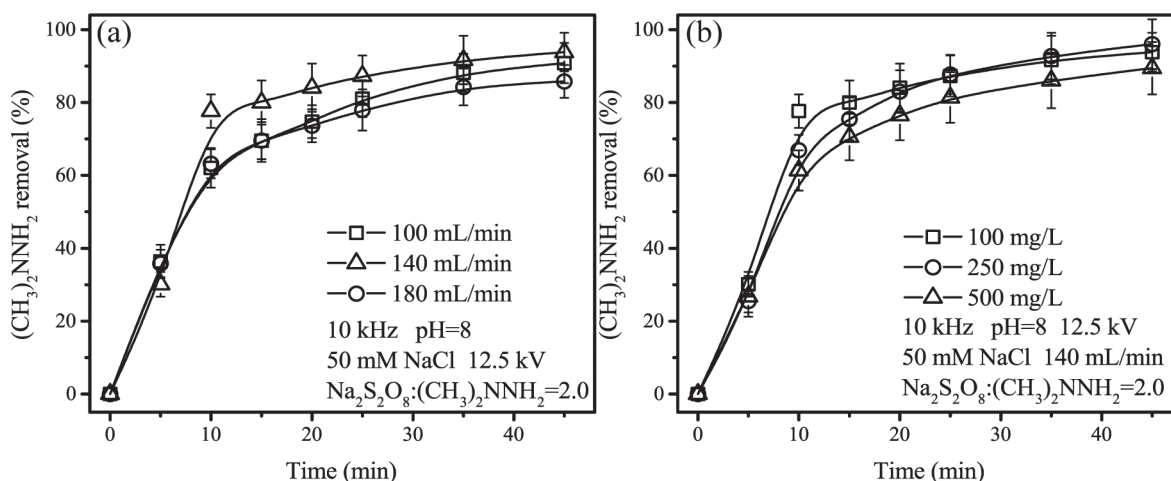


Fig. 5. a) Oxidizing kinetics of UDMH in with variation of circular flow. b) Oxidizing kinetics of UDMH in different UDMH concentration.

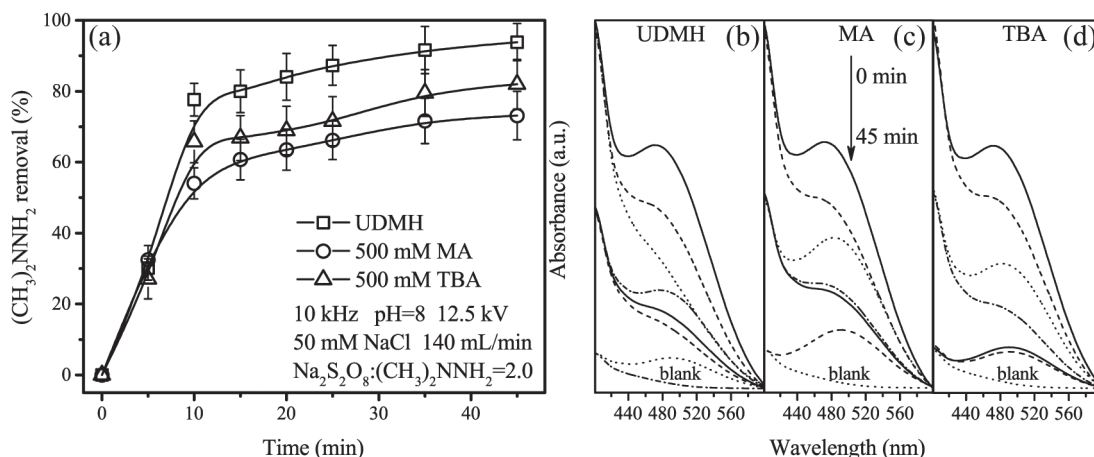


Fig. 6. a) Decomposition capacity of UDMH with time after adding MA and TBA. (b-d) UV-vis spectra of solution before and after MA and TBA addition.

50 mM NaCl, pH 8, and 12.5 kV. As can be seen, the oxidizing kinetics of 100-500 mg/L UDMH manifested marginal difference in degradation efficiency and removal rate, alluding to the stability of persulfate-plasma strategy.

Free Radicals Quenching Test

Quenching test was carried out to evaluate the predominant radicals as depicted in Fig. 6. Similar oxidizing test was implemented by replacing ultrapure water with 500 mM methanol (MA) and tertiary-butyl alcohol (TBA) solution while maintaining other parameters unchanged.

TBA and MA is an efficacious dissipation to $\cdot\text{OH}$ and $\cdot\text{SO}_4^-/\cdot\text{OH}$, severally [28]. After addition TBA, the elimination percentages of UDMH inhibited from 77.6% to 65.8% within 10 min. Whereas UDMH removal was suppressed to 54.0% in 10 min reaction after MA competition. Difference between TBA and MA addition hinting that $\cdot\text{SO}_4^-$ participated in UDMH decomposition. After 45 min plasma treatment, $\sim 70\%$ UDMH was devastated in MA solution, authenticating a non-radical oxidation process [32]. Direct oxidation by persulfate and plasma-engendered O_3 played a role in UDMH elimination.

A decreasing peak at the spectral range of 450-550 nm as a function of time in Fig. 6b) corresponded to the UDMH. During the UDMH degradation, the intensity of UDMH was decelerated gradually with the competition of TBA and MA (Fig. 6c-d). In line with our quenching test, UV-vis spectra illustrated that UDMH remediation hinged on synergistic effect between $\cdot\text{OH}$ and $\cdot\text{SO}_4^-$.

Conclusions

In sum, a hybrid DBD plasma/persulfate treatment device were fabricated in UDMH wastewater purification. Water chemistry experiments, UV-vis spectroscopy, and the Visual MINTEQ simulation were performed to investigate the oxidizing behaviors of UDMH in this integrated system. Moreover, the influence of peak voltage, $\text{Na}_2\text{S}_2\text{O}_8$ -to-UDMH molar ratios, initial pH, ionic strength, circular flow, and UDMH concentration on UDMH elimination were systematically exhibited. The parameters obtained from water chemistry experiments were successfully removed 93.8% UDMH in 45 min, following the optimum condition: $\text{Na}_2\text{S}_2\text{O}_8/\text{UDMH}$ (mol/mol) = 2, 50 mM NaCl, 12.5 kV, pH = 8, and 140 mL/min. Mechanisms about predominating reactive oxygen species during UDMH degradation were revealed in the assistant of radical scavengers. The $\cdot\text{OH}$ and $\cdot\text{SO}_4^-$ played a synergistic role in the UDMH oxidization. The insights gained from our investigations highlight the magnitude of application-oriented combination strategy in industry wastewater remediation.

Acknowledgments

This study was subsidized by the Market Regulation Science and Technology Program, China (No. 2022MK181) and the National Institute of Metrology, China (No. AKYZZ2234 and BH2107).

Conflict of Interest

The authors declare no conflict of interest.

References

- HE X.Z. Natural purification of shuttle thrust agent wastewater at site. *Pollut. Control Technol.* **9** (2), 69, **1996**.
- ZHENG M., CHEN X., CHENG R., LI N., SUN J., WANG X., ZHANG T. Catalytic decomposition of hydrazine on iron nitride catalysts. *Catal. Commun.* **7** (3), 187, **2006**.
- DENG X.S., LIU X.X., LIU Y., CAO L.W. Progress in treatment technology of unsymmetrical dimethylhydrazine wastewater. *Chem. Propellants Polym. Mater.* **13** (3), 21, **2015**.
- NWANKWOALA A.U., EGIEBOR N.O., NYAVOR K. Enhanced biodegradation of methylhydrazine and hydrazine contaminated NASA wastewater in fixed-film bioreactor. *Biodegrad.* **12** (1), 1, **2001**.
- ZENG B.P., JIA Y., XU G.G., LI M., FENG R. Preparation of $\text{TiO}_2/\text{g-C}_3\text{N}_4$ by CTAB-assisted and photocatalytic degradation of unsymmetrical dimethylhydrazine waste water. *J. Mater. Eng.* **47** (9), 139, **2019**.
- YU Y., ZHOU Z., ZHANG C., SONG X., SONG X., ZHANG Z. Antimony speciation on a dithiothreitol-functionalized two-dimensional Au@Ag array by surface-enhanced Raman spectroscopy. *Sens. Actuators, B.* **373**, 132607, **2022**.
- GU D., GUO C., LV J., HOU S., ZHANG Y., FENG Q., ZHANG Y., XU J. Removal of methamphetamine by UV-activated persulfate: Kinetics and mechanisms. *J. Photochem. Photobiol., A.* **379**, 32, **2019**.
- YU Y., ZHOU Z., SONG X., SONG X., ZHANG Z., JING C. Mechanistic insights into dual active sites in Au@W18O49 electrocatalysts for the hydrogen evolution reaction. *Inorg. Chem. Front.* **9** (18), 4785, **2022**.
- YU Y.Q., ZHOU Z., DING Z.X., ZUO M.M., CHENG J.M., JING C.Y. Simultaneous arsenic and fluoride removal using $\{201\}\text{TiO}_2\text{-ZrO}_2$: Fabrication, characterization, and mechanism. *J. Hazard. Mater.* **377**, 267, **2019**.
- HAN Y., HUANG M.J., ZHOU T., WU X.H. Interfacial reaction mechanism of copper oxide activating persulfate. *Environ. Chem.* **39** (3), 735, **2020**.
- WANG X., WANG Y., CHEN N., SHI Y., ZHANG L. Pyrite enables persulfate activation for efficient atrazine degradation. *Chemosphere*, **244**, 125568, **2020**.
- ZHOU Z., ZHANG X., ZHANG T., MA W., FANG X. UV-activated peroxymonosulfate for haloacetamides degradation: Kinetics and reaction pathways. *J. Dispers. Sci. Technol.* **43** (3), 399, **2022**.
- SON G., LEE H. Methylene blue removal by submerged plasma irradiation system in the presence of persulfate. *Environ. Sci. Pollut. Res.* **23** (15), 15651, **2016**.
- SHANG K.F., LI W.F., WANG X.J., LU N., JIANG N., LI J., WU Y. Degradation of p-nitrophenol by DBD plasma/

- Fe²⁺/persulfate oxidation process. *Sep. Purif. Technol.* **218**, 106, **2019**.
15. LIU H.Y., SONG Z.Q., SONG C., WANG S.G. The simultaneous removal of Cr (VI) and phenol by non-thermal plasma. *Ind. Water Treat.* **40** (4), 35, **2020**.
 16. RONG J.F., LI L.Y., HE Y., ZHANG Y., LI F.H., SHI T.S. Study on efficient purification of PAM wastewater by non-thermal plasma. *New Chem. Mater.* **48** (3), 269, **2020**.
 17. CHEN J., FENG J., LU S., SHEN Z., DU Y., PENG L., NIAN P., YUAN S., ZHANG A. Non-thermal plasma and Fe²⁺ activated persulfate ignited degradation of aqueous crystal violet: Degradation mechanism and artificial neural network modeling. *Sep. Purif. Technol.* **191**, 75, **2018**.
 18. QIU C.Y., GUAN X.T., LIU Z., ZHU A.N., YAN K.P. Degradation of organic dyes by nanosecond pulsed discharge plasma. *High Power Laser Part. Beams.* **32** (2), 025010, **2020**.
 19. WANG Q.C., ZHANG A., LI P., HEROUX P.H., ZHANG H., YU X., LIU Y.A. Degradation of aqueous atrazine using persulfate activated by electrochemical plasma coupling with microbubbles: Removal mechanisms and potential applications. *J. Hazard. Mater.* **403**, 124087, **2021**.
 20. BOUKARI S.O.B., PELLIZZARI F., KARPEL VEL LEITNER N. Influence of persulfate ions on the removal of phenol in aqueous solution using electron beam irradiation. *J. Hazard. Mater.* **185** (2), 844, **2011**.
 21. FENG J., JIANG L., ZHU D., SU K., ZHAO D., ZHANG J., ZHENG Z. Dielectric barrier discharge plasma induced degradation of aqueous atrazine. *Environ. Sci. Pollut. Res.* **23** (9), 9204, **2016**.
 22. LIU Y., QU G.Z., SUN Q.H., JIA H.Z., WANG T.C., ZHU L.Y. Endogenously activated persulfate by non-thermal plasma for Cu (II)-EDTA decomplexation: Synergistic effect and mechanisms. *Chem. Eng. J.* **406**, 126774, **2021**.
 23. HOEBEN W.F.L.M., VANOOIJ P.P., SCHRAM D.C., HUISKAMP T., PEMEN A.J.M., LUKEŠ P. On the possibilities of straightforward characterization of plasma activated water. *Plasma Chem. Plasma Process.* **39** (3), 597, **2019**.
 24. HAYON E., SIMIC M. Intermediates produced from one-electron oxidation of hydrazine - Evidence for formation and decay of tetrazane and triazene. *J. Am. Chem. Soc.* **94** (1), 42, **1972**.
 25. KOLTHOFF I.M., MILLER I.K. The chemistry of persulfate. I. The kinetics and mechanism of the decomposition of the persulfate ion in aqueous medium. *J. Am. Chem. Soc.* **73** (7), 3055, **1951**.
 26. FAN Y., JI Y., KONG D., LU J., ZHOU Q. Kinetic and mechanistic investigations of the degradation of sulfamethazine in heat-activated persulfate oxidation process. *J. Hazard. Mater.* **300**, 39, **2015**.
 27. GAO L., SUN L., WAN S., YU Z., LI M. Degradation kinetics and mechanism of emerging contaminants in water by dielectric barrier discharge non-thermal plasma: The case of 17β-Estradiol. *Chem. Eng. J.* **228**, 790, **2013**.
 28. YUAN S., LIAO P., ALSHAWABKEH A.N. Electrolytic manipulation of persulfate reactivity by iron electrodes for trichloroethylene degradation in groundwater. *Environ. Sci. Technol.* **1** (48), 656, **2014**.
 29. SHANG K., LI W., WANG X., LU N., JIANG N., LI J., WU Y. Degradation of p-nitrophenol by DBD plasma/Fe²⁺/persulfate oxidation process. *Sep. Purif. Technol.* **218** (1), 106, **2019**.
 30. ZAREI A.R., REZAEIVAHIDIAN H., SOLEYMANI A.R. Mineralization of unsymmetrical dimethylhydrazine (UDMH) via persulfate activated by zero valent iron nano particles: modeling, optimization and cost estimation. *Desalin. Water Treat.* **57** (34), 16119, **2016**.
 31. WANG X.P., MEI J. Removal of TBBPS from simulated production wastewater by bubble film dielectric barrier discharge plasma. *Chin. J. Environ. Eng.* **15** (7), 2305, **2021**.
 32. WANG Y.F., LI Y.B., WANG Y.B., QI P.J., ZHAO K. Oxidation destruction of Cu (CN)₃²⁻ by persulfate. *Environ. Sci.* **38** (3), 1061, **2017**.